

Physicochemical characterization and in vitro behavior of daunorubicin-loaded poly(butylcyanoacrylate) nanoparticles

Margarita Simeonova^{a,b,*}, Galya Ivanova^c, Venelin Enchev^c, Nadezhda Markova^c,
Mihail Kamburov^a, Christo Petkov^d, Aoife Devery^e, Robert O'Connor^e,
Dermot Brougham^{e,f}

^a Department of Polymer Engineering, University of Chemical Technology and Metallurgy, 8 Kliment Ohridski Blvd., 1756 Sofia, Bulgaria

^b Institute of Polymers, Bulgarian Academy of Sciences, Acad. G. Bonchev Str. bl. 103A, 1113 Sofia, Bulgaria

^c Institute of Organic Chemistry, Bulgarian Academy of Sciences, Acad. G. Bonchev Street bl 9, 1113 Sofia, Bulgaria

^d Central Custom Laboratory, 47 Rakovski Street, 1040 Sofia, Bulgaria

^e National Institute for Cellular Biotechnology, Dublin City University, Dublin 9, Ireland

^f School of Chemical Sciences, Dublin City University, Dublin 9, Ireland

Received 4 August 2008; received in revised form 29 December 2008; accepted 14 January 2009

Available online 31 January 2009

Abstract

The design, preparation and characterization of poly(butylcyanoacrylate) nanoparticles as a drug-delivery system for daunorubicin is reported. A range of light scattering [photon correlation spectroscopy (PCS)], spectroscopic [¹H nuclear magnetic resonance (¹H NMR), Fourier transform infrared (FTIR), chromatographic [gel permeation chromatography (GPC)] and quantum chemical techniques have been employed for the physicochemical characterization of drug-loaded nanoparticles and to clarify the mechanisms of drug immobilization in the polymer matrix. The presence of daunorubicin in the polymerization medium was found to affect both the degree of polymerization and the compactness of the resulting nanoparticles. The GPC, FTIR and ¹H NMR results confirmed cytostatic immobilization in the polymer matrix, with evidence for the presence of three types of inclusion: physically entrapped, polymer-associated (due to hydrogen bonds and/or dipole-charge interactions with the polymer chains), and polymer surface-adsorbed daunorubicin. The developed colloidal delivery system has the capacity for sustained in vitro release of daunorubicin. Preliminary in vitro assays were carried out on two cell lines, DLKP and DLKP-A, which display different levels of drug resistance, to evaluate the cytotoxicity of the drug-loaded nanoparticles.

© 2009 Acta Materialia Inc. Published by Elsevier Ltd. All rights reserved.

Keywords: Poly(butylcyanoacrylate) nanoparticles; Drug delivery system; Daunorubicin; DLKP and DLKP-A cell lines; Cytotoxicity

1. Introduction

Anthracycline antibiotics rank among the most effective anticancer drugs ever developed [1,2]. After more than 40 years, the parent anthracyclines, doxorubicin (Dox) and daunorubicin (Dau) (Fig. 1), continue to be essential com-

ponents of first-line chemotherapy in the treatment of a variety of solid and hematological malignancies [3]. Despite this activity, anthracyclines are hugely toxic agents, hence methods that improve their therapeutic index would greatly increase their utility and efficacy. The treatment of patients with anthracyclines alone or in combination with other drugs is generally complicated by high incidence of hematological and cardiac toxicity. Anthracyclines are also used as substrates for cellular drug efflux pumps, such as P-glycoprotein (P-gp) (MDR-1), a protein commonly overexpressed on cancer cell membranes, which makes cells resistant to therapy with substrate drugs, including many

* Corresponding author. Address: Department of Polymer Engineering, University of Chemical Technology and Metallurgy, 8 Kliment Ohridski Blvd., 1756 Sofia, Bulgaria. Tel.: +359 2 8163 226.

E-mail addresses: msimeonova@uctm.edu, simeonova.margarita@gmail.com (M. Simeonova).

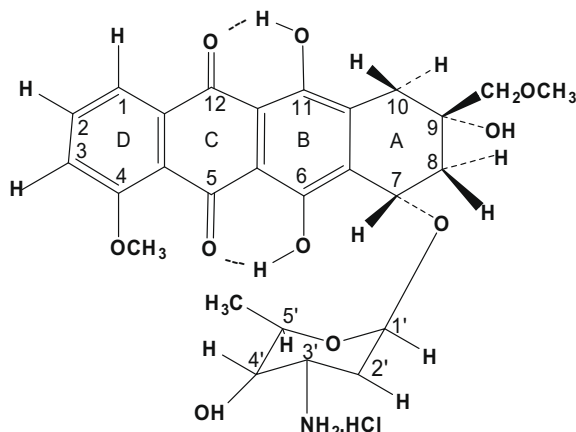


Fig. 1. Molecular structure of Dau. The tautomer presented, one of four available, provides the closest agreement of the calculated chemical shift values with experimental results (Table 1).

important anti-cancer agents, by reducing the amount of drug getting into the cell. P-gp is a major cause of this form of resistance, termed multiple drug resistance (MDR). Strategies for improving the efficacy and/or cardiac safety of current anthracyclines have generally utilized two medicinal chemistry approaches: (i) the development of new analogs; and (ii) the development of tumor-targeted formulations.

Anthracyclines consist of a planar aglycon chromophore bearing an amino sugar ring (Fig. 1). The search for new compounds revealed a direct structure–activity relationship between the aglycon and/or the amino sugar chemical structure and activity [4]. Slight structural modifications can lead to reduced cardiotoxicity, and can alter the extent and spectrum of anti-tumour activity. Daunorubicin is more effective in the treatment of leukemia [5], while the closely related doxorubicin is more effective in the treatment of solid tumors [6].

The pharmacological strategies for achieving tumor-targeted delivery of anthracyclines may be classified into two main groups [7]: (i) development of carriers that assist their preferential distribution within tumors; and (ii) conjugation of anthracyclines to a carrier that specifically binds to tumor cells. Liposomal and nanoparticulate formulations of Dox or Dau offer best examples of pharmaceutical developments of the first strategy. Various forms of polymer-bound Dox offer good examples of pharmaceutical developments of the second strategy [2].

It has been shown that polymer nanoparticles have a great potential for anticancer drug delivery and tumor targeting [8]. Biocompatible and biodegradable poly(alkylcyanoacrylate) (PACA) nanoparticles have been proposed as anthracycline delivery vehicles to overcome the two main problems of cumulative cardiotoxicity and drug resistance, which limit the clinical use and efficacy of anthracycline antibiotics [9–15]. Preclinical studies have demonstrated the ability of poly(isohexylcyanoacrylate) nanoparticles to reduce the cardiotoxicity of Dox by mod-

ifying its tissue distribution [9]. Doxorubicin, incorporated into PACA nanoparticles, has been investigated in different resistant cell lines [10–14]. It has been shown that the association of Dox with PACA nanoparticles overcame the resistance to Dox in a large number of MDR cell lines [12]. The nanoparticle-associated Dox accumulated within the MDR cells and appeared to avoid, or at least partially overcome, P-gp-dependent efflux. This reversal was only seen with PACA nanoparticles and was not observed to be due to endocytosis of the nanoparticles. Rather, the formation of a complex between positively charged Dox and negatively charged polymer degradation products such as poly(alkylcyanoacrylic acid) seemed to favor the diffusion across the cell membrane [11]. However, the exact mechanism by which Dox-nanoparticles bypass the MDR mediated by P-gp remains unclear.

Surprisingly, given the strong interest in clinical application of these carrier systems, to the best of our knowledge there have been no experimental studies published on the modes of interaction of anthracyclines with PACA. The only relevant work is a computational study which demonstrated the feasibility of interactions between Dox and PACA [16]. However, experimental studies of the anthracycline inclusion may provide critical insight for the development of tailored drug delivery vehicles. The aim of the study reported here is both to examine the practical potential of poly(butylcyanoacrylate) nanoparticles (PBCN) as a delivery system for Dau and to assess the molecular events leading to drug immobilization in the polymer matrix. Furthermore, a preliminary *in vitro* investigation of the cytotoxic potential of drug-loaded nanoparticles was carried out using two human squamous non-small cell lung carcinoma cell lines to evaluate cell-line-specific differences in the degree of resistance to chemotherapy. The cell lines chosen were DLKP [17,18], a poorly differentiated human squamous cell lung carcinoma, and DLKP-A [19], a highly resistant clone of DLKP which overexpresses the P-gp drug efflux pump.

2. Materials and methods

2.1. Materials

The monomer normal-butyl-2-cyanoacrylate (*n*-BCA) was obtained from the Research Centre for Specialty Polymers, Bulgaria. Dextran 40 (mol. wt. 40 kDa) was obtained from Pharmachim (Bulgaria) and citric acid from POCH (Poland). Daunorubicin hydrochloride was purchased from Fluka. Other chemicals were of laboratory grade purity and used as obtained.

2.2. Preparation and purification

2.2.1. Preparation of unloaded PBCN

Poly(butylcyanoacrylate) nanoparticles were prepared using open anionic polymerization of *n*-butyl-2-cyanoacrylate monomer in an aqueous medium, acidified by citric

acid (0.2% w/v), containing dextran 40 (0.8% w/v) as a steric colloidal stabilizer and without addition of an emulsifier. Polymerization was carried out for 3 h under magnetic agitation and room temperature. The resulting polymer colloidal suspension (20 mg ml^{-1}) was then adjusted to pH 7 using 1N NaOH.

2.2.2. Preparation of Dau-loaded nanoparticles

Daunorubicin loading of nanoparticles was accomplished during the polymerization process by entrapment of the drug into the formed polymer matrix. Powdered Dau, in appropriate amounts up to 5 mg ml^{-1} , was dissolved in the polymerization medium and the monomer n-BCA (20 mg ml^{-1}) was subsequently instilled carefully into the mixture. The polymerization was then carried out under the same conditions as the unloaded nanoparticles. The pH of the Dau-PBCN suspensions was adjusted to 7 with aqueous 1 N NaOH.

2.2.3. Preparation of solution of free Dau

Freeze-dried powdered Dau was dissolved in aqueous polymerization medium at appropriate concentrations and the pH of the solutions obtained was raised to neutrality with 1 N NaOH.

2.2.4. Purification of Dau-loaded and unloaded nanoparticles suspensions

To perform gel permeation chromatography (GPC), Fourier transform infrared (FTIR) and nuclear magnetic resonance (NMR) analyses, the polymer suspensions were dialyzed against distilled water, using cellulose Visking membrane (MWCO 12,000–14,000: pore diameter 25 \AA) (Serva, USA) at room temperature for 24 h to remove agents such as dextran, citric acid or free drug that were dissolved in the polymer medium.

2.3. Physicochemical characterization

2.3.1. Particle size determination

The diameter of nanoparticles was determined by photon correlation spectroscopy (PCS). The dynamic light scattering experiments were performed on a high-performance particle sizer (HPPS; Malvern Instruments, Malvern, UK) using a detection angle of 173° at a temperature of 25°C . The HPPS uses a 3 mW He–Ne laser operating at a wavelength of 633 nm. The z-average diameters (mean hydrodynamic diameter based upon the intensity of scattered light) and the polydispersity index (PDI) values (an estimate of the distribution width) were calculated from the Cumulants analysis as defined in ISO13321 [20].

2.3.2. Gel permeation chromatography

GPC was carried out using a Waters GPC system fitted with refractive index (Waters R401) and ultraviolet (UV) spectrophotometric (Waters 486) detectors coupled for simultaneous double detection. Three ultra-Styrigel col-

umns with nominal pore sizes of 100 \AA , 1000 \AA and linear were used simultaneously. Tetrahydrofuran (THF) was used as an eluent, with a flow rate of 1 ml min^{-1} , at 45°C . Sample solutions were prepared by dissolving 14–16 mg of dried nanoparticles in 4 ml of THF and filtering through a $0.45 \mu\text{m}$ filter. Quantities of each solution ($200 \mu\text{l}$) were injected into the chromatographic system. The chromatograms were recorded using simultaneous double detection; UV absorbance was monitored at a wavelength of 254 nm. Elution volumes were referenced to toluene as an internal standard. Calibration was carried out with polystyrene standards.

2.3.3. Drug loading determination (indirect estimation)

The degree of Dau incorporation into the polymer matrix of nanoparticles was determined spectrophotometrically using a Perkin Elmer Lambda 2 UV/VIS spectrometer, after filtration of portions of intact drug-loaded polymer suspensions over a $0.1 \mu\text{m}$ pore sized membrane. Drug concentration in the filtrate was determined by direct spectrophotometric analysis at $\lambda_{\text{max}} = 482 \text{ nm}$. The amount of drug incorporated into the nanoparticle matrix was determined after subtracting unincorporated drug amount from total known amount of drug added. The entrapment efficiency and drug loading capacity were calculated by:

%entrapment efficiency

$$= 100 \times \frac{\text{initial concentration} - \text{concentration in filtrate}}{\text{initial concentration}}$$

loading capacity

$$= \frac{\text{amount of drug incorporated in nanoparticles (mg)}}{\text{polymer mass (mg)}}$$

2.3.4. Fourier transform infrared spectroscopy

FTIR spectra of the nanoparticles (with and without drug) or Dau were recorded in KBr pellets on a Perkin Elmer 1000 FTIR spectrometer with resolution of 2 cm^{-1} . A total of 64 scans were used and data were recorded over the range $4000\text{--}400 \text{ cm}^{-1}$.

2.3.5. ^1H NMR spectroscopy

NMR spectra of Dau, unloaded PBCN and Dau-loaded PBCN were recorded on a Bruker DPX 400 spectrometer operating at 400 MHz, using a 5 mm z-gradient probe and deuterated dimethyl sulfoxide ($\text{DMSO-}d_6$) as a solvent. ^1H NMR spectra of 3.8 mM (2 mg ml^{-1}) and 38 mM (20 mg ml^{-1}) Dau in $\text{DMSO-}d_6$ were measured. Proton NMR spectra of Dau-loaded PBCN in $\text{DMSO-}d_6$, at a temperature of 300 K and different drug concentrations (0.8, 1.0, 2.0, 3.0 and 5.0 mg ml^{-1}), were measured. Standard one-dimensional (1-D) ^1H NMR experiments with 30° pulses, acquisition time 4.09 s and a relaxation delay of 2 s were performed. A total of 256 transients with a spectral width of 6000 Hz were collected into 32 K time domain

points. The solvent resonance peak at 2.49 ppm (DMSO- d_6) was used as a chemical shift reference. Two-dimensional $^1\text{H}/^1\text{H}$ correlation spectroscopy (COSY) and $^1\text{H}/^1\text{H}$ total correlation spectroscopy (TOCSY) were acquired using standard Bruker software. Magnitude mode ge-2-D-COSY spectra incorporating a double quantum filter, gradient pulses for selection with a gradient ratio of 16:12:40 and a relaxation delay of 2 s were performed. A total of 2000 data points in F_2 and 256 data points in F_1 were collected over a spectral width of 5000 Hz. $^1\text{H}/^1\text{H}$ TOCSY spectra were recorded using MLEV-17 sequence with a mixing time of 80 ms; 2000 data points were collected, with a spectral width of 6000 Hz and a relaxation delay of 2 s. A total of 256 data points were collected in F_1 , using either 16 or 32 transients and 16 dummy scans.

2.3.6. Quantum chemical calculations

Four tautomeric forms of neutral Dau, their complexes with one DMSO molecule and three dimeric structures of Dau were considered. Semi-empirical PM3 (for dimers) and ab initio HF/3-21G quantum chemical calculations were carried out. Local minima were verified by frequency analysis. To obtain more accurate energies, single-point ab initio calculations at the HF/6-31G**//HF/3-21G level were performed. All calculations were carried out using the GAMESS quantum chemistry package [21]. To estimate the effect of the polar medium on the relative stabilities of the Dau tautomers and their complexes we applied the polarizable continuum model [22,23] as implemented in the GAUSSIAN 98 [24] suite of programs at the HF/6-31G** level for the geometries optimized at the HF/3-21G level of theory. The proton chemical shieldings were calculated using the gauge-including atomic orbitals (GIAO) approach [25,26] at the HF/6-31G** level. For comparison with experimental results, the calculated absolute shieldings were transformed to chemical shifts using the reference compound tetramethylsilane (TMS): $\delta = \delta_{\text{calc}}(\text{TMS}) - \delta_{\text{calc}}$. Both $\delta_{\text{calc}}(\text{TMS})$ and δ_{calc} were evaluated with the same method and basis set. The NMR calculations were carried out using GAUSSIAN 98.

2.4. Performance evaluation of drug–nanoparticle formulations

2.4.1. In vitro drug release

Appropriate amounts of Dau-loaded nanoparticles samples containing 1, 2 or 3 mg ml $^{-1}$ of drug were enclosed in a dialysis bag, sealed and placed in a vessel containing 25 ml of the incubation medium [phosphate-buffered saline (PBS), pH 7.4] and maintained under constant mild agitation in a water bath (37 °C). The final concentration of Dau was chosen to ensure sink conditions for the in vitro study. Aliquots (1.5 ml) were taken, and subsequently replaced, in predetermined time intervals from 10 to 540 min. Each aliquot was analyzed with UV–visible spectroscopy at 482 nm for Dau content as described above.

2.4.2. In vitro cytotoxicity

A proliferation method was used to determine the cytotoxicity of the preparations towards DLKP and DLKP-A cell lines. Cytotoxicity testing of drugs was measured by the acid phosphatase assay as previously described [27,28]. Briefly, cells were seeded at 1×10^3 cells well $^{-1}$ in a 96-well plate and left to attach overnight in a 5% CO $_2$ incubator at 37 °C. The appropriate concentrations of drug/nanoparticle formulations were prepared freshly at twice their final concentration and added to the plate on the following day. The assay was terminated after a further 7-day incubation. The effect of treatment was examined by comparing the growth of cells in the treated rows to the growth of cells in the control rows and expressing these as a percentage. All assays were performed at least in triplicate.

3. Results

3.1. Physical characterization

3.1.1. Nanoparticle morphology and loading

The anionic polymerization of *n*-butylcyanoacrylate led to the formation of various populations of oligomers including tetramers, hexamers and octamers [29]. The GPC profile of unloaded PBCN (not presented here) indicates the presence of oligomeric chains with a mol. wt. of 1084 ($n = 9$). Polymerization in the presence of Dau (2 mg ml $^{-1}$) resulted in oligomeric chains with lower molecular weight (468), suggesting a lower degree of polymerization ($n = 4$) of the oligomeric molecules that form the nanoparticles. The *z*-average hydrodynamic diameter (D_{hyd}) of the unloaded nanoparticles determined by PCS was 192 nm (PDI = 0.05), while the values for the Dau-loaded nanoparticles were 183 (0.07), 156 (0.05) and 125 (0.06), for the 2, 3 and 5 mg ml $^{-1}$ Dau, respectively. The very low PDI values confirm that the suspensions are highly size-monodisperse, hence the differences in the measured D_{hyd} values are significant. The smaller drug-loaded

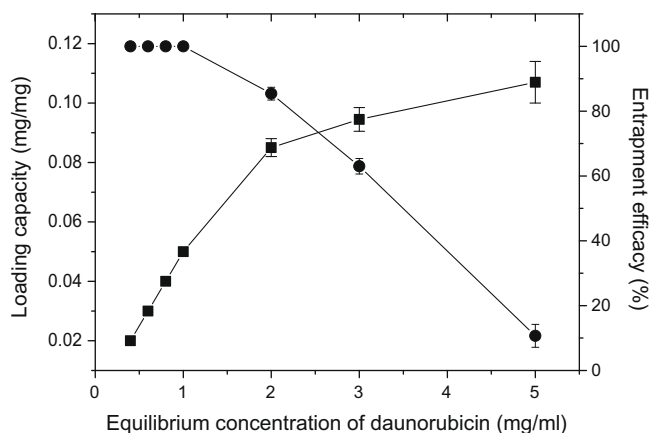


Fig. 2. Dependence of the loading capacity (■) and entrapment efficiency (●) on drug concentration used during the preparation.

nanoparticles are associated with the presence of shorter polymer chains.

The ability of a nanoparticulate system to transport significant quantities of the drug is critical for reducing the quantity of carrier required to achieve therapeutic concentrations. For this reason, the loading capacity and entrapment efficiency of the PACA–Dau system were studied by indirect spectrophotometric analysis. The results are presented in Fig. 2. When Dau was dissolved in the polymerization medium in the concentration range of 0.4–1 mg ml⁻¹, 100% entrapment efficiency was observed. Presumably in this concentration range the drug is entrapped within the polymer matrix of the formed nanoparticles according to the mechanism of aggregation [16] with loadings in the 0.02–0.05 mg mg⁻¹ range. On increasing the equilibrium drug concentration the entrapment efficiency decreases, but loading capacities in the range of 0.08–0.11 mg mg⁻¹ were obtained. This strongly suggests the presence of different modes of inclusion for equilibrium concentrations in excess of 1 mg ml⁻¹. From the inclusion perspective, the optimal formulation is obtained at the cross-over point, i.e. when a concentration little over of 2 mg ml⁻¹ of drug is used in the polymerization medium (Fig. 2).

3.2. Molecular characterization

3.2.1. FTIR spectroscopy

FTIR studies were performed to confirm drug insertion into the nanoparticles. In the FTIR spectrum of Dau (Fig. 3), two strong bands of similar intensity are observed at 1617 and 1580 cm⁻¹. The first is due to the C=O stretching mode of hydrogen-bonded quinone carbonyl groups and the second, to the C=C stretching mode [30]. The absorption patterns are generally affected by the presence

of intramolecular hydrogen-bonding systems involving the quinone carbonyl groups. In the situation where both carbonyl groups are involved in hydrogen bonding with the perihydroxyl (Fig. 1), two bands of similar intensity appear near 1620 and 1580 cm⁻¹ [31]. In addition, the absence of a band near at 1670 cm⁻¹ confirms that both anthraquinone carbonyl groups are hydrogen bonded [30].

The FTIR spectrum of PBCN (Fig. 3) shows the CH₃ (ν_{as}) at 2964 cm⁻¹, CH₂ (ν_{as}) at 2938 cm⁻¹ and CH₃ (ν_s) at 2876 cm⁻¹. The characteristic C≡N stretching mode of the polymer was observed at 2250 cm⁻¹. The prominent band at 1748 cm⁻¹ corresponds to the C=O stretching mode, while the features at 1258 and 1018 cm⁻¹ correspond to the asymmetric and symmetric C–O–C stretches, respectively. The CC≡N (ν_s) band was observed at 1167 cm⁻¹.

In the FTIR spectrum of Dau-PBCN (Fig. 3) two characteristic bands assigned to the stretching of hydrogen-bonded quinone carbonyl groups at 1617 cm⁻¹ (slightly more intense) and to the C=C stretching at 1580 cm⁻¹ were observed. This is strong evidence for the presence of drug molecules in the polymer matrix. The characteristic bands of poly(butylcyanoacrylate) remain unchanged, with the exception of the band assigned to CC≡N, which shifted from 1167 to 1171 cm⁻¹ and the band assigned to C–O–C (ν_s), which shifted from 1018 to 1015 cm⁻¹. For the former, the shift probably arises due to a dipole-charge interaction between the polymer cyano group and the amino group of Dau, while the latter shift is probably due to a weak dipole-charge interaction between the polymer ester carbonyls and the hydroxyl groups of the amino sugar.

3.2.2. ¹H NMR spectroscopy

NMR spectroscopy was employed to study the drug–polymer interactions. One- and two-dimensional (¹H/¹H

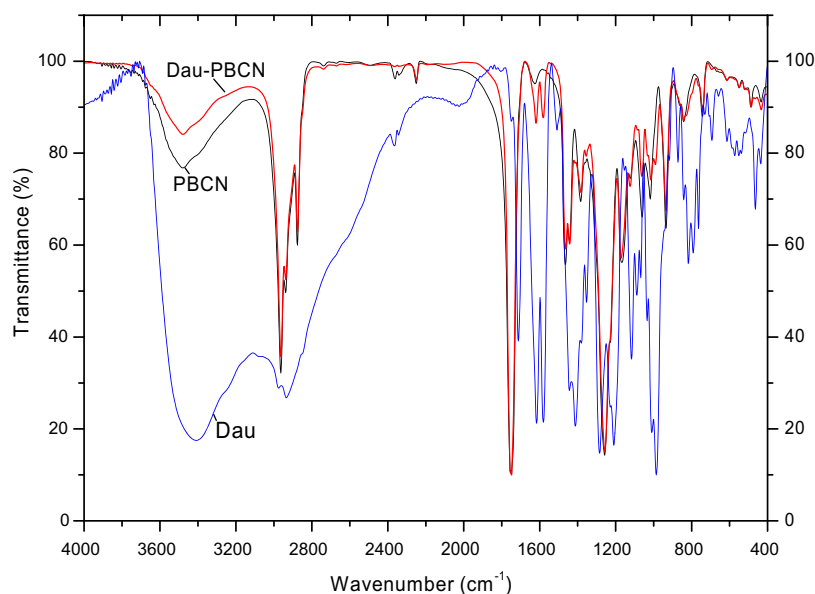


Fig. 3. FTIR spectra recorded in KBr for PBCN, free Dau and Dau – PBCN.

COSY and $^1\text{H}/^1\text{H}$ TOCSY) NMR spectra of Dau, Dau-loaded PBCN (Dau-PBCN) and unloaded PBCN in $\text{DMSO-}d_6$ were recorded. Typical ^1H spectra are shown in Fig. 4. The signal assignment, based on an analysis of the 1- and 2-D spectra, is presented in Table 1. Additionally, ^1H NMR spectra of PBCN loaded with different drug concentrations in $\text{DMSO-}d_6$ were measured to investigate the behavior, and in particular the aggregation, of Dau. The results for free Dau are largely in agreement with the previous literature [32–35], where all data were recorded in D_2O , with only a few minor changes in chemical shift. Thus it is reasonable to compare the chemical shift changes for Dau-PBCN with the literature values of Dau, this substitution was necessary given the solubility of the drug-polymer conjugate.

^1H NMR spectra of Dau-loaded nanoparticles, prepared with a range of drug concentrations (0.8, 1.0, 2.0, 3.0 and 5.0 mg ml^{-1}) in $\text{DMSO-}d_6$ at 300 K, were recorded (Fig. 5). The spectra are dominated by the intense and broad resonance signals of the polymer chain, Table 1. Resonances arising from drug included in the polymer nanoparticles were clearly observed. In the 1-D ^1H and 2-D $^1\text{H}/^1\text{H}$ COSY spectra, three resonances can be identified for each of the following Dau protons: H6' (doublets at 1.21, 1.16 and 1.13 ppm), H5' (4.20, 4.18 and 4.0 ppm) and COCH_3 (2.30, 2.26 and 2.24 ppm).

3.2.3. Quantum chemical calculations

To clarify the molecule structure and conformational behavior of neutral Dau, we considered its four tautomeric forms, their complexes with a single DMSO molecule and three dimers of Dau. The geometry optimizations for the dimers were carried out at semi-empirical level using the PM3 method. These calculations suggest that intermolecular hydrogen bonding between two Dau molecules is not possible because the $\text{H} \cdots \text{O}$ distances obtained were greater than 5 \AA and dimmer could not form. The reason is the presence of a methyl group close to carbonyl oxygen atom (unlike to Dox), which sterically hinders the site.

Daunorubicin can theoretically exist in four tautomeric forms: **A**, **B**, **C** and **D** (Fig. 6). The geometry optimizations at the ab initio HF/3-21G level suggest that the tautomer **A** is most stable in the gas phase followed by tautomer **C**, which is $0.97 \text{ kcal mol}^{-1}$ less stable (Table 2). Species **B** and **D** are more than 11 kcal mol^{-1} less stable than tautomer **A**. The picture changes when single-point calculations at the HF/6-31G^{**}//HF/3-21G level are performed. In this case, the most stable tautomer is **C**. The energy difference between **C** and **A** is 1 kcal mol^{-1} . The same situation is observed when the effect of the polar medium (DMSO) on the relative stabilities of the Dau tautomers is taken into account, i.e. PCM/HF/6-31G^{**}//HF/3-21G calculations.

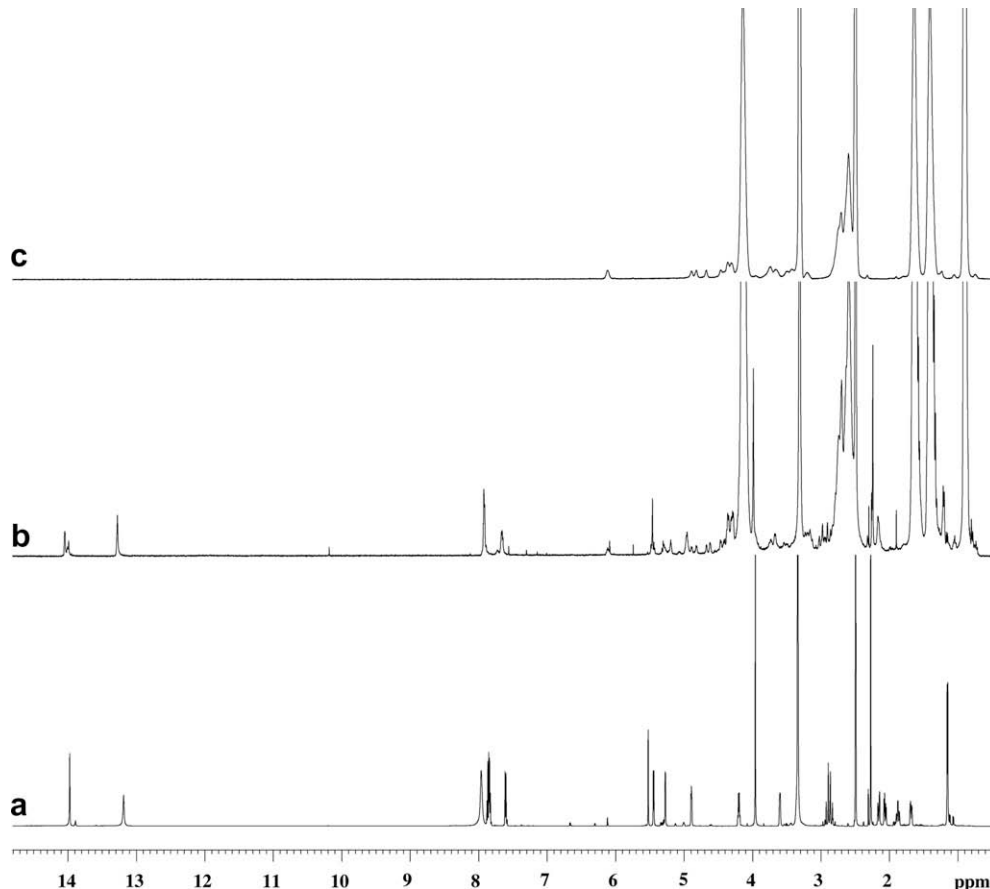


Fig. 4. 400 MHz ^1H NMR spectra in $\text{DMSO-}d_6$ of (a) Dau, (b) Dau-loaded PBCN and (c) unloaded PBCN.

Table 1
Chemical shifts (δ , ppm) and assignment of the 400 MHz ^1H NMR spectra of Dau, Dau-loaded PBCN and unloaded PBCN in $\text{DMSO}-d_6$, at 300 K.

Proton	Dau, 20 mg ml^{-1} (38 mM)	Dau, 2 mg ml^{-1} (3.8 mM)	Unloaded PBCN	Dau- loaded PBCN
<i>Daunorubicin</i>				
H-1	7.83	7.92		7.89 ^a
H-2	7.87	7.91		7.89 ^a
H-3	7.61	7.66		7.63
H-7	4.88	4.94		4.93
H-8a	2.05	2.1		2.1
H-8e	2.15	2.16		2.15
H-10a	2.84	2.93		2.91 ^a
H-10e	2.91	2.93		2.91 ^a
OCH_3	3.95	3.98		3.97
C(O)CH_3	2.27 (2.30)	2.26		2.30 (2.26, 2.24)
H-1'	5.27	5.29		5.29
H-2'a	1.67	1.68		1.68 ^a
H-2'e	1.87	1.88		1.88
H-3'	3.35	3.36		3.37
H-4'	3.59	3.56		3.54
H-5'	4.2	4.19		4.20 (4.18, 4.0)
H-6'	1.15 (1.06, 1.11)	1.15		1.16 (1.21, 1.13)
OH-4'	5.46	5.43		5.43
OH-9	5.53	5.5		5.45
OH-6	13.19, <i>11.42</i> , 12.74	13.26		13.26
OH-11	13.97, <i>13.70</i> , 13.97	14.03		14.04
NH_2	7.97	7.83		7.74
<i>PBCN</i>				
$\text{O}-\text{CH}_2\text{CH}_2-$			4.13	4.13
$-\text{CH}_2-$			2.59	2.6
$\text{CH}_3\text{CH}_2\text{CH}_2-$			1.62	1.63
CH_3CH_2-			1.41	1.4
CH_3			0.89	0.89

For the numbering of the atoms see Fig. 1. The OH-6 and OH-11 GIAO calculated chemical shifts for tautomer **C** (Fig. 6) are presented in italics and those for structure **CS1** (Fig. 7) are given in bold.

^a Daunorubicin associated with the polymer chains by H-bonds and/or dipole-charge interactions.

The solvent effect was also simulated using the supermolecular approach. In this approach one molecule of DMSO is attached to each molecule of the four tautomers. For this purpose, two regions in the Dau molecule were considered, labeled S1 and S2 (Fig. 7). Because of the large size of molecule investigated, the influence of only a single DMSO solvent molecule, situated in the S1 or S2 region, was studied. Surprisingly, the **DS2** complex of Dau is predicted to be the most stable at all the computational levels considered (Table 2). The stability sequence of the complexes is **DS2** > **CS1** > **AS1** > **AS2** at all levels of theory. A significant decrease in the energy differences between the tautomeric forms is observed when the effect of the medium (DMSO) is included in the calculations. Hence, the exis-

tence of two or three tautomeric forms in DMSO is probable (Table 2).

The HF/6-31G** GIAO calculated proton chemical shifts of the three most stable tautomeric forms and their complexes with one DMSO molecule were compared to the experimentally obtained values. The chemical shifts of tautomer **C** and complex **CS1** of Dau calculated at the HF level without taking into account the solvent effect are closer to the NMR experimental data (Table 1), suggesting that this is the dominant tautomer.

3.3. Performance evaluation of drug–nanoparticle formulations

3.3.1. In vitro drug release

The in vitro drug release from Dau-loaded nanoparticles was monitored as a function of time in PBS buffer at pH 7.4. We observed strong dependence of the drug release profile on the drug loading of the nanoparticles (Fig. 8). The 1 mg ml^{-1} drug–nanoparticle formulation (100% entrapment efficiency; the entire drug is included in the nanoparticles) did not release measurable quantities of Dau over a 9 h period. On the other hand, the release profiles of the 2 mg ml^{-1} (optimal) and the 3 mg ml^{-1} formulations show significant release over a timescale of several hours. There was a gradual reduction in the rate of release for both of these formulations, although neither was observed to reach an obvious plateau (no further release) over the time of the study.

3.3.2. Toxicity in cell culture

The potential of PBCN to be used as a carrier for Dau was evaluated in vitro, by comparing the cytotoxicity of four formulations: unloaded nanoparticles (PBCN), 20 mg ml^{-1} ; free Dau in solution (Dau), 2 mg ml^{-1} ; Dau-loaded nanoparticles (Dau–PBCN) (at the same concentrations as the unloaded nanoparticles and free Dau); and a physical mixture of Dau and unloaded nanoparticles (Dau + PBCN). The in vitro models chosen for investigating the potential of these materials were the parent DLKP and resistant daughter DLKP-A cell lines. The experiments confirmed that PBCN has minimal cytotoxicity in the range used in this study. The growth inhibition of the Dau-containing formulations was tested at concentrations ranging from 1 to 50 nM for the DLKP cell line, and at concentrations ranging from 1 to 800 nM for the highly resistant DLKP-A cell line (Fig. 9).

Drug-concentration-dependent decreases in cell viability were observed for both lines. In the case of DLKP, this was at a much lower concentration. However, the association of Dau with nanoparticles does not markedly improve their effectiveness towards the two resistant cell lines as compared to the free drug. The concentration required to reduce the cell proliferation by 50%, the IC_{50} value, was calculated. The IC_{50} s for Dau alone and in combination with the nanoparticles

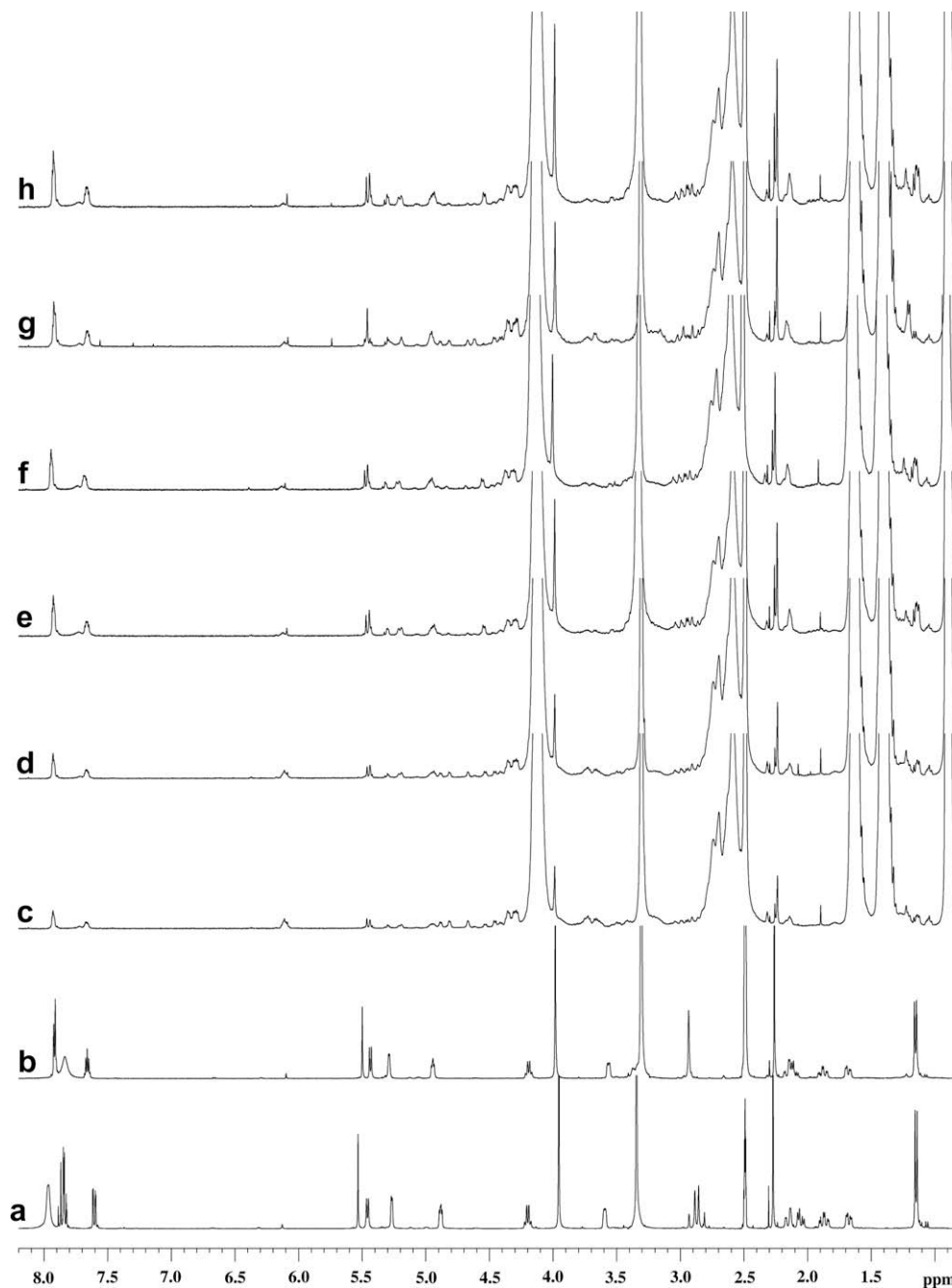


Fig. 5. Selected spectral area of ^1H NMR spectra in $\text{DMSO}-d_6$ at 300 K of (a) Dau (20 mg ml^{-1} , 38 mM), (b) Dau (2 mg ml^{-1} , 3.8 mM), (c) Dau-loaded PBCN (Dau = 0.8 mg ml^{-1}), (d) Dau-loaded PBCN (Dau = 1.0 mg ml^{-1}), (e) Dau-loaded PBCN (Dau = 2.0 mg ml^{-1}), (f) Dau-loaded PBCN (Dau = 3.0 mg ml^{-1}), (g) Dau-loaded PBCN (Dau = 3.0 mg ml^{-1} , after dialysis) and (h) Dau-loaded PBCN (Dau = 5.0 mg ml^{-1}).

(Dau–PBCN and Dau + PBCN) were 15 and 25 nM for DLKP and 380 and 450 nM for DLKP-A cells. As expected, higher IC_{50} values were observed for the resistant daughter cell-line, probably due to the higher expression of P-gp, which is highly efficient at pumping anthracyclines such as Dau out of the cell. It is also interesting that the Dau–PBCN formulation deviated from the expected behavior, in that it was less effective at higher dosages in the case of DLKP-A, but not for DLKP.

4. Discussion

4.1. Physical characterization

4.1.1. Nanoparticle morphology and loading

The reduced size of the drug-loaded nanoparticles may be due to: (i) change in the particle compactness due to a strong intermolecular interaction between the drug and polymer; or (ii) change in the aggregation number of polymer molecules. Indeed, the smaller size of the loaded nano-

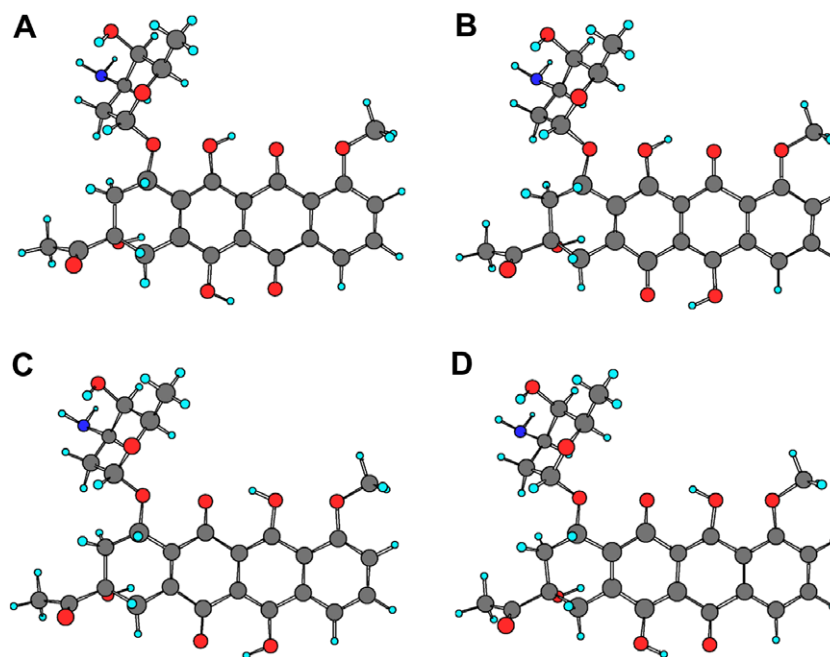


Fig. 6. HF/3-21G optimized structures of the solvated tautomeric forms **A**, **B**, **C** and **D** of Dau.

particles suggests a possible role of drug–polymer interactions in particle formation. The cohesion forces operating in the drug–polymer matrix arise from a blend of: (i) dipole-charge interactions, including strong interactions between the protonated ammonium group of the amino sugar and the cyano groups and a weaker interaction between the ester carbonyls of the PBCN and hydroxyl

groups on the amino sugar; (ii) potential hydrogen bonds, again between the ammonium function and the cyano groups; and (iii) hydrophobic forces [16].

The NMR analysis of Dau–PBCN suggests the presence of three forms of Dau in the nanoparticles matrix. Broadening of the resonances was observed for the signals of two of the suggested forms. It is likely that this arises due to exchange broadening from H-bonds between the Dau and polymer and/or dipole-charge interactions. The observed decrease in the intensity of the most downfield shifted resonances after dialysis of Dau–PBCN indicates that these resonances can be assigned to Dau weakly adsorbed on or near the surface of the polymer nanoparticles (Fig. 5f and g). Further support for this assignment comes from the fact that the intensity of these resonances was greater for the samples prepared at higher equilibrium drug concentrations. However, attempting quantification is not appropriate as broadening suggests variation in T_2 , which may suppress some of the ^1H magnetization into the baseline. Finally, for the galactosamine group, the observation of a broad resonance signal for the amino protons and the fact that the other chemical shifts (e.g. of $\text{H}3'$) were unchanged suggests that there is no direct bonding interaction between this group and the polymer matrix.

A number of investigations have demonstrated that in both buffered and unbuffered aqueous solutions Dau undergoes self-association, due to stacking of the anthracycline aromatic rings, with observed concentration and temperature dependencies [32,34,35]. ^1H NMR spectra of Dau in $\text{DMSO}-d_6$ at two concentrations (38 and 3.8 mM) were recorded to investigate this possibility. An upfield chemical shift was observed at the higher concentration for the resonances belonging to the anthracycline residue, i.e.

Table 2

Calculated relative energies, ΔE_{r} , in kcal mol^{-1} , for Dau tautomers (Fig. 6) and for the most stable DMSO complexes of Dau tautomers (Fig. 7) at different computational levels: PM3, HF/3-21G, HF/6-31G**//HF/3-21G and PCM/HF/6-31G**//HF/3-21G.

Structures (Fig. 6)	ΔE_{r}	Structures (Fig. 7)	ΔE_{r}
PM3		PM3	
A	0	AS1 + DMSO	2.32
B	10.37	AS2 + DMSO	0
C	7.35	CS1 + DMSO	10.92
D	10.7	DS2 + DMSO	6.26
HF/3-21G		HF/3-21G	
A	0	AS1 + DMSO	8.61
B	11.76	AS2 + DMSO	7.93
C	0.97	CS1 + DMSO	2.41
D	11.26	DS2 + DMSO	0
HF/6-31G**//HF/3-21G		HF/6-31G**//HF/3-21G	
A	1.01	AS1 + DMSO	2.36
B	11.99	AS2 + DMSO	5.27
C	0	CS1 + DMSO	0.85
D	12.22	DS2 + DMSO	0
PCM/HF/6-31G**//HF/3-21G		PCM/HF/6-31G**//HF/3-21G	
A	0.46	AS1 + DMSO	1.71
B	11.8	AS2 + DMSO	4.7
C	0	CS1 + DMSO	1.6
D	2.29	DS2 + DMSO	0

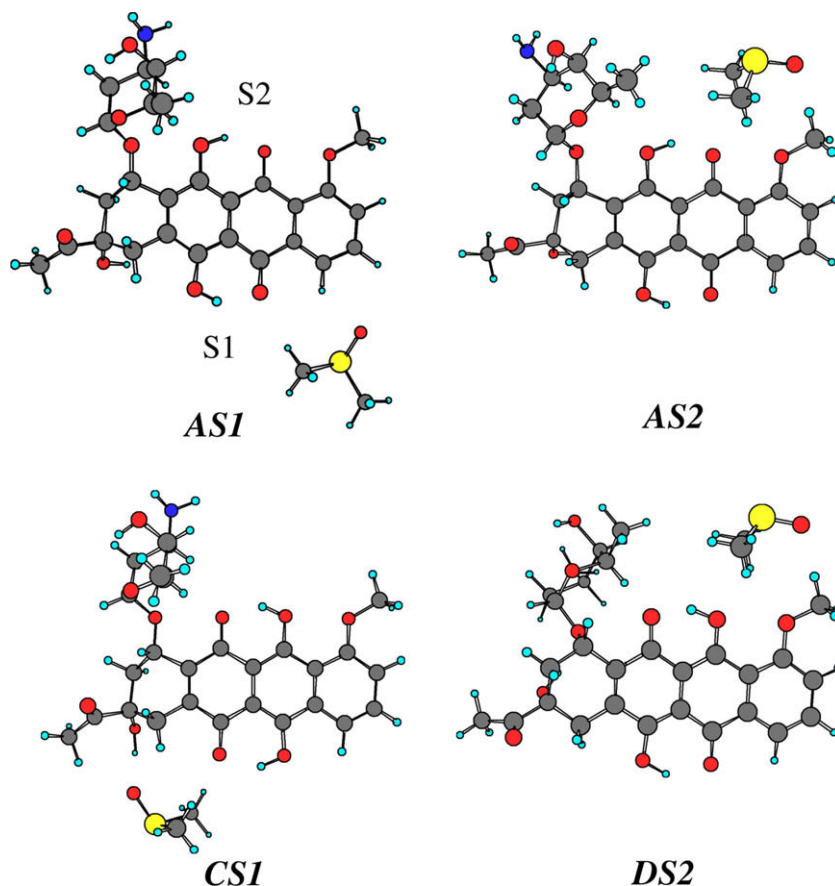


Fig. 7. HF/3-21G optimized structures of the most stable DMSO complexes of Dau tautomers.

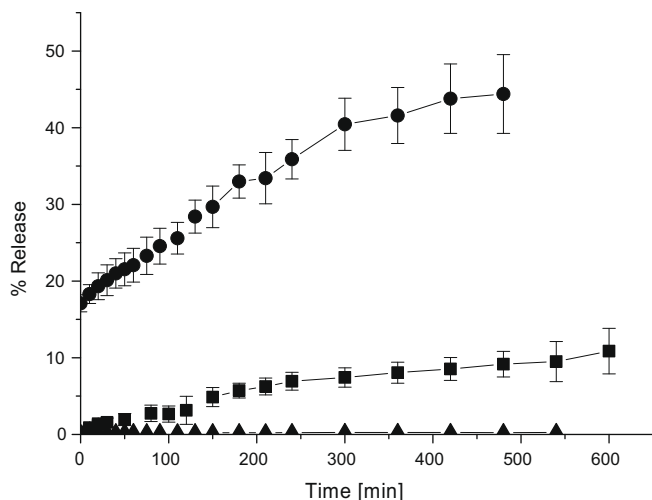


Fig. 8. Drug releases profile of Dau-PBCN suspensions prepared with 3 mg ml⁻¹ (●), 2 mg ml⁻¹ (■) and 1 mg ml⁻¹ (▲) equilibrium drug concentration.

H-1, H-2, H-3, H-7, H-8a and H-10a (Table 1), but not for H-8e and H-10e, which can thus be assigned to the side of the molecule pointing into solution. From the ¹H NMR spectra we can deduce that Dau exists as an aggregated form in DMSO solution at high concentrations (38 mM) as a result of the stacking of the anthracylene ring system

based on dipole-charge interactions. We can thus assign the resonances labeled H-8e and H-10e to the side of the dimer pointing into solution. The coincidence of the chemical shifts of the protons of Dau molecules in the spectra of Dau-PBCN with those in the spectra of 3.8 mM Dau suggests that the molecule is included as a monomer, at the low concentrations relevant to this study.

Thus the NMR analysis strongly suggests the presence of three types of Dau in the polymer matrix of nanoparticles, in the probable order of strength of interaction with the matrix: (i) bound Dau, which interacts directly with the polymer chains due to H-bonds and/or dipole-charge interactions; (ii) physically entrapped Dau; and (iii) adsorbed Dau, associated with the accessible surfaces of the nanoparticles. It is likely that type I Dau influences the nanoparticle formation most strongly. One could speculate that during polymerization the oligomeric poly(butylcyanoacrylate)s scavenge the amphiphilic Dau from the aqueous phase into the progressively more lipophilic phase of the growing poly(butylcyanoacrylate) chains [16]. Evidently, the inclusion of Dau into this phase leads to a decrease in the degree of polymerization of the oligomeric molecules, which is probably not surprising if one considers that at an equilibrium drug concentration of 1 mg ml⁻¹ the molar ratio of Dau/monomer is 0.0135. As more Dau is added, the degree of polymerization decreases, so in a

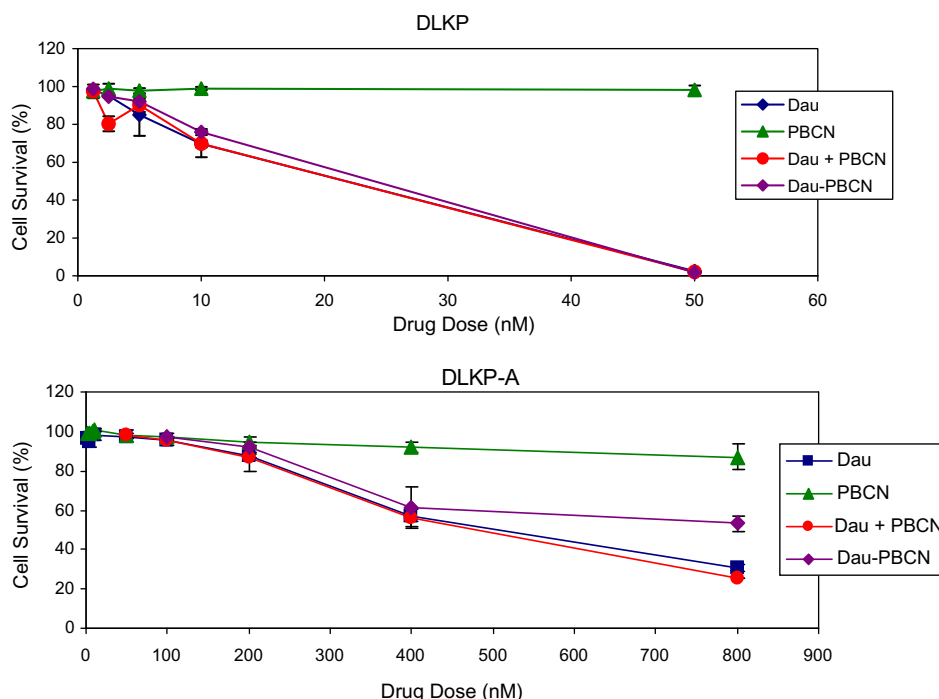


Fig. 9. Cytotoxicity range of the Dau formulations against the DLKP (upper) and DLKP-A (lower) cell lines. The suspensions of Dau-loaded PBCN were prepared with a 2 mg ml^{-1} equilibrium concentration (equivalent to 3.8 mM), which was diluted as required.

180–190 nm nanoparticle there will be an increase in the number of polymer chains, which is apparently associated with an increase in the loading capacity, mostly due to the inclusion of more physically trapped Dau. The entrapment efficiency continues to decrease with increased equilibrium Dau concentration, as progressively more of the potential inclusion sites (of all three types) are occupied.

4.2. Performance evaluation of drug–nanoparticle formulations

The temporal drug release profile from nanoparticles is usually biphasic; an initial burst is followed by a period of slow sustained release. We observed a fast release of a limited quantity of Dau for the formulation obtained with a 3 mg ml^{-1} initial concentration of the drug (Fig. 8). We attribute this to the liberation of surface localized and loosely associated drug (type III Dau). For this formulation, nearly 17% of the encapsulated drug was rapidly released, corresponding to about 0.015 mg of the 0.095 mg mg^{-1} (Dau/polymer) encapsulated. For the 2 mg ml^{-1} formulation, about 0.085 mg mg^{-1} Dau was included, which suggests that a very small quantity was adsorbed in this case. After about 10 min, both the 2 and 3 mg ml^{-1} formulations exhibit a slow sustained rate of release over many hours, of a significant fraction of the remaining $0.07\text{--}0.08 \text{ mg mg}^{-1}$ of Dau. The higher 3 mg ml^{-1} formulation shows a faster release rate over the time range studied. For both samples we interpret the faster rate observed up to about 270 min as arising predominantly from loss of type III (adsorbed) Dau. After this

time the rate decreases, as only types I and II Dau remain. The decrease in rate over the full time course suggests that at higher equilibrium drug concentrations there is more type II and III drug included. The faster rates observed at 3 mg ml^{-1} are as expected, since when the size of these pools of Dau are increased, the strength of interaction with the same quantity of polymer decreases.

Negligible quantities of Dau were released from the 1 mg ml^{-1} formulation. Given the 100% entrapment efficiency obtained for this formulation, 0.05 mg Dau incorporated for every 1 mg of monomer is retained as type I Dau. This is due to strong interactions between Dau and the polymer matrix, so Dau release would require hydrolytic erosion of the polymer. In the case of PBCN this would involve hydrolysis of the ester side groups, decreasing the hydrophobic interactions arising from water intrusion and increasing repulsive forces between the anionic carboxylates [16]. Similarly, both higher concentration formulations retain at least 0.05 mg mg^{-1} of Dau over the entire 9 h period. It is not easy to quantify how much Dau is included in this form, given the absence of a long-time plateau for these samples.

The effect of the prolonged retention is manifested in the *in vitro* behavior of Dau–PBCN with the DLKP-A cell line in particular. For DLKP there is no observed difference in cell survival between free Dau and Dau–PBCN at all dosages used, while for the resistant DLKP-A the picture is somewhat different. First, even at very high concentrations cell survival never falls to $\sim 0\%$. Secondly, a higher percentage of the cells survive with Dau–PBCN than with the other treatments. This is strong evidence for the long-term retention of significant quantities of Dau in the nanopartic-

ulate carrier for extended periods in the immediate cellular environment, if not within the cells themselves. This is an interesting observation, as the development of systems that reduce the drug burst while maintaining their integrity in biological systems remains an important goal for the drug delivery community.

5. Conclusions

This work presents a complete experimental approach to the design and preparation of Dau-loaded poly(butylcyanoacrylate) nanoparticles, by polymerization of *n*-butylcyanoacrylate monomer in the presence of Dau. It was found that the presence of the amphiphilic drug molecules during the polymerization reaction reduces the degree of polymerization of the polymer as well as the size (compactness) of the simultaneously formed nanoparticles. The results obtained by NMR studies strongly suggest that Dau was included in three forms: associated with the polymer chain by H-bonds and/or dipole-charge interactions; physically entrapped in the polymer matrix; and adsorbed on the surface of nanoparticles. Due to the presence of these different modes of inclusion, the nanoparticulate drug delivery system has the potential for sustained delivery/release of Dau in vitro.

The biological performance of the obtained Dau-nanoparticle formulations is still at an early stage since in this paper we have concentrated on their design and characterization. We plan to perform a detailed biological examination of these formulations, such as new in vitro examinations with other tumor cell lines and in vivo examinations on systemic drug toxicity.

References

- [1] Weiss RB. The anthracyclines: will we ever find a better doxorubicin? *Semin Oncol* 1992;19:670–86.
- [2] Minotti G, Menna P, Salvatorelli E, Cairo G, Gianni L. Anthracyclines: molecular advances and pharmacologic developments in antitumor activity and cardiotoxicity. *Pharmacol Rev* 2004;56:185–229.
- [3] Lothstein L, Israel M, Sweatman TW. Anthracycline drug targeting: cytoplasmic versus nuclear – a fork in the road. *Drug Resist Update* 2001;4:169–77.
- [4] Arcamone F. *Medicinal Chemistry*, vol. 7. New York: Academic Press; 1981.
- [5] Paciucci PA, Cuttner J, Gottlieb A, Davies RB, Martelo O, Molland JF. Sequential mitoxantrone, daunorubicin and cytosine arabinoside for patients with newly diagnosed acute myelocytic leukemia. *Am J Hematol* 1997;56:214–8.
- [6] Di Marco A, Arcamone F, Zunino F. In: Corcoran JW, Hahn FE, editors. *Antibiotics*. Berlin: Springer Verlag; 1974. p. 101–28.
- [7] Perez-Soler R, Sugarman S, Zou Y, Priebe W. Anthracycline antibiotics, new analogues, methods of delivery and mechanisms of action. *Am Chem Soc Symp Ser* 1995;574:300–19.
- [8] Kreuter J. Nanoparticles – a historical perspective. *Int J Pharm* 2007;331:1–10.
- [9] Kattan J, et al. Phase I clinical trial and pharmacokinetic evaluation of doxorubicin carried by polyisohexylcyanoacrylate nanoparticles. *Invest New Drugs* 1992;10:191–9.
- [10] Nemati F, Dubernet C, Fessi H, de Verdière Colin A, Poupon MF, Puisieux F, et al. Reversion of multidrug resistance using nanoparticles in vitro: influence of the nature of the polymer. *Int J Pharm* 1996;38:237–46.
- [11] de Verdière C, et al. Reversion of multidrug resistance with polyalkylcyanoacrylate nanoparticles: towards a mechanism of action. *Br J Cancer* 1997;76:198–205.
- [12] Soma CE, Dubernet C, Barratt G, Némati F, Appel M, Benita S, et al. Ability of doxorubicin-loaded nanoparticles to overcome multidrug resistance of tumor cells after their capture by macrophages. *Pharm Res* 1999;16:1710–6.
- [13] Soma CE, Dubernet C, Bentolia D, Benita S, Couvreur P. Reversion of multidrug resistance by co-encapsulation of doxorubicin and cyclosporin A in polyalkylcyanoacrylate nanoparticles. *Biomaterials* 2000;21:1–7.
- [14] Aquali N, Morjani H, Trussardi A, Soma E, Giroux B, Manfait M. Enhanced cytotoxicity and nuclear accumulation of doxorubicin-loaded nanospheres in human breast cancer MCF7 cells expressing MRP1. *Int J Oncol* 2003;23:1195–201.
- [15] Vauthier C, Dubernet C, Chauvierre C, Brigger I, Couvreur P. Drug delivery to resistant tumors: the potential of poly(alkyl cyanoacrylate) nanoparticles. *J Control Release* 2003;93:151–60.
- [16] Poupart HJ, Couvreur P. A computationally derived structural model of doxorubicin interacting with oligomeric polyalkylcyanoacrylate in nanoparticles. *J Control Release* 2003;92:19–26.
- [17] Law E, Gilvarry U, Lynch V, Gregory B, Grant G, Clynes M. Cytogenetic comparison of two poorly differentiated human lung squamous cell carcinoma lines. *Cancer Genet Cytogenet* 1992;59:111–8.
- [18] Duffy CP, et al. Enhancement of chemotherapeutic drug toxicity to human tumour cells in vitro by a subset of non-steroidal anti-inflammatory drugs (NSAIDs). *Eur J Cancer* 1998;34:1250–9.
- [19] Heenan M, O'Driscoll L, Cleary I, Connolly L, Clynes M. Isolation from a human MDR lung cell line of multiple clonal subpopulations which exhibit significantly different drug resistance. *Int J Cancer* 1997;71:907–15.
- [20] International Standard ISO13321. Methods for determination of particle size distribution part 8: photon correlation spectroscopy. Geneva: International Organization for Standardization; 1996.
- [21] Schmidt MW, et al. General atomic and molecular electronic structure system. *J Comput Chem* 1993;14:1347–63.
- [22] Miertus S, Scrocco E, Tomasi J. Electrostatic interaction of a solute with a continuum. A direct utilization of ab initio molecular potentials for the prevision of solvent effects. *Chem Phys* 1981;55:117–29.
- [23] Tomasi J, Mennucci B, Cancès E. The IEF version of the PCM solvation method: an overview of a new method addressed to study molecular solutes at the QM ab initio level. *J Mol Struct (THEO-CHEM)* 1999;464:211–26.
- [24] Frisch MJ, et al. *Gaussian 98*, revision A.7. Pittsburgh, PA: Gaussian, Inc.; 1998.
- [25] Ditchfield R. Self-consistent perturbation theory of diamagnetism. I. A gauge-invariant LCAO (Linear Combination of Atomic Orbitals) method for NMR chemical shifts. *Mol Phys* 1974;27:789–807.
- [26] Wolinski K, Hilton JF, Pulay P. Efficient implementation of the gauge-independent atomic orbital method for NMR chemical shift calculations. *J Am Chem Soc* 1990;112:8251–60.
- [27] Martin A, Clynes M. Acid phosphatase: endpoint for in vitro toxicity tests. *In Vitro Cell Dev Biol* 1991;27A(3 Pt 1):183–4.
- [28] Touhey S, O'Connor R, Plunkett S, Maguire A, Clynes M. Structure–activity relationship of indomethacin analogues for MRP-1, COX-1 and COX-2 inhibition. Identification of novel chemotherapeutic drug resistance modulators. *Eur J Cancer* 2002;38:1661–70.
- [29] Beham N, Birkinshaw C, Clarke N. Poly *n*-butyl cyanoacrylate nanoparticles: a mechanistic study of polymerization and particle formation. *Biomaterials* 2001;22, 1335–1334.
- [30] Bloom H, Briggs LH, Cleverley B. Physical properties of anthraquinone and its derivatives. Part 1. Infrared spectra. *J Chem Soc* 1959:178–85.
- [31] Vigevari A, Ballabio M, Gandini E, Penco S. ¹H NMR and IR spectra of antitumour anthracyclines: effect of the substitution pattern

- on the chemical shift values of the phenolic protons and on IR absorptions of the quinone system. *Magn Res Chem* 1985;23:344–52.
- [32] Chaires JB, Dattagupta N, Crothers DM. Self-association of daunomycin. *Biochemistry* 1982;21:3927–32.
- [33] Barthwal R, Mujeeb A, Srivastava N, Sharma U. A proton nuclear magnetic resonance investigation of the conformation of daunomycin. *Chem Biol Interact* 1996;100:125–39.
- [34] Davies DB, Evstigneev MP, Veselkov DA, Veselkov AN. Hetero-association of anticancer antibiotics in aqueous solution: NMR and molecular mechanics analysis. *Biophys Chem* 2005;117:111–8.
- [35] Evstigneev MP, Khomich VV, Davies DB. Self-association of daunomycin antibiotic in various buffer solutions. *Russ J Phys Chem* 2006;80:741–6.